XI CONGRESSO NACIONAL DE ENGENHARIA MECÂNICA
DE 07 A 11 DE AGOSTO DE 2022, TERESINA-PI, BRASIL

ON THE TOPOLOGY OPTIMIZATION OF 2D-SWIRL FLOW STATOR AND ROTOR PROBLEMS WITH BINARY DESIGN VARIABLES

Anderson Soares da Costa Azevêdo, anderson.sca@usp.br[1]
Eduardo Moscatelli, emoscatelli@usp.br[1]
Shahin Ranjbarzadeh, ranjbarzadeh@usp.br[1]
Emílio Carlos Nelli Silva, ecnsilva@usp.br[1]
Renato Picelli, rpicelli@usp.br[1]

[1]Polytechnic School of the University of São Paulo, São Paulo, Brazil

Abstract: *One considerable challenge for the topology optimization of fluids is the solution of 3D (three-dimensional) problems. Since solving a 3D fluid flow topology optimization problem is costly, the development of 2D swirl flow frameworks is of high interest. Regarding engineering applications, topology optimization considering the swirl flow can be applied to obtain innovative designs in rotating machinery devices like labyrinth seals. The seal mechanism consists of two parts, a stator and a rotor separated by a gap, which provides a tortuous path to minimize the fluid leakage. In this work, we employ the TOBS-GT (Topology Optimization of Binary Structures with Geometry Trimming) method to solve a 2D axisymmetric seal problem considering two distinct rotational velocities on solid material. We maximize the fluid flow energy dissipation subjected to a minimum gap between stator and rotor material phases of the seal model. The 2D swirl flow is governed by the Navier-Stokes equations in the inertial reference frame. The governing equations are solved via the Finite Element Method considering axisymmetry and the optimization problem is solved by using sequential integer linear programming. In order to avoid jagged geometries, which affects the accuracy of turbulence modelling, we adopt an additional step to create a smooth wall representation. The numerical example shall elucidate how the rotational speed and minimum gap influences on swirl flow path evolution and on final stator and rotor design for low Reynolds regime. Finally, the TOBS-GT shows to be an improved method to create of new topologies for rotating machinery devices.*
Keywords: *Topology optimization, Laminar flow, Turbomachinery, TOBS method, Integer Linear Programming*

1. INTRODUCTION

The growing demand for lower pollutant emissions and more efficient devices lead the interest of industries to reduce the gas leakage on rotating machinery devices like labyrinth seals. Particularly, this fluid diode mechanism has the function of sealing rotating parts subjected to high pressure from fluid flow between the shaft and stator parts. In this quest, topology optimization emerges as a potential engineering tool to obtain innovative designs considering the three phases (rotor, stator and fluid) of this complex problem. The complexity begins in the scope of numerical analysis, since the evaluation of flow patterns and design of effective topologies may need to address unsteady flow behavior with strong jets, flow detachment and presence of vortex (Fraczek and Wróblewski, 2016). Fluid flow topology optimization was introduced in Borrvall and Petersson (2003) pursuing the path with minimum energy dissipation assuming a Stokes flow. Ever since, topology optimization of fluid flow problems has been approached through several methodologies, from: i) density; ii) binary; and iii) level set methods. Regarding topology optimization on fluid flow with binary variables $\{0, 1\}$, remarkably advances started recently in this decade via the TOBS method. Souza *et al.* (2021) extended the TOBS method to fluid flow optimization considering laminar flow and demonstrated the feasibility of the procedure via three benchmark fluid literature problems. The standard TOBS (without trimming) was proposed by Sivapuram and Picelli (2018) as a method capable to achieve optimum structures design using discrete variables and formal mathematical programming. More recently, Picelli *et al.* (2022) inaugurated the TOBS-GT procedure to fluid flow optimization considering turbulent flow in 2D and 3D problems. One year later, Moscatelli *et al.* (2022) proposed a topology optimization formulation capable of solving 2D swirl fluid flow problems composed with different velocities via a TOBS-based approach.

In this paper we formulated the stator and rotor problem considering two design variable and a proper mapping between both solid and fluid phases considered on the 2D swirl flow problem. We demonstrate our approach with TOBS-GT in a benchmark seal example. Numerical results show to signify the influence of rotational speed and minimum gap on final designs and total energy dissipation achieved.

2. 2D SWIRL LAMINAR FLUID FLOW

In this paper, we consider a stator and rotor problem that presents symmetry around an axis. In order to reduce the computational cost, we adopt cylindrical coordinates and solve the problem on the axisymmetric domain developing a 2D swirl flow model. Fig. 1 illustrates the relation between the coordinates of a cartesian O_{xyz} and a cylindrical frame $O_{r\phi z}$ from the a) 3D and b) 2D axisymmetric model.

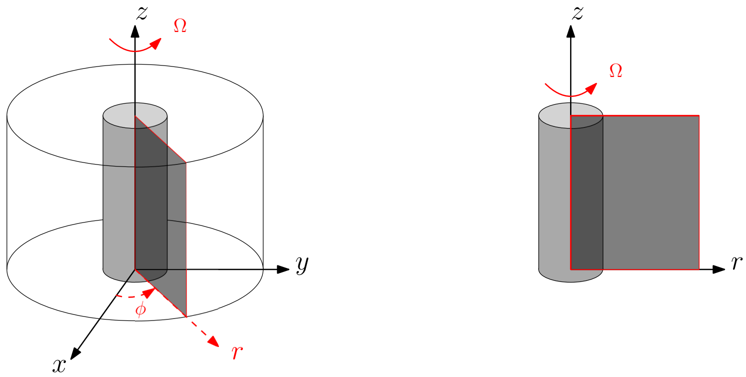

(a) Cartesian and cylindrical coordinates system (b) Modeled region (r-z plane)

Figure 1: **Rotating coordinates system.**

Regarding the cylindrical reference frame, two cases may be considered: i) inertial; or ii) non-inertial (rotational). In both cases the governing equations are derived considering continuity and momentum equations. However, the difference rest in the observed velocity on the reference frame: absolute or relative for inertial and non-inertial, respectively. Also, two additional body forces (centrifugal and Coriolis) emerge on the momentum equations for the rotational reference frame. In this work, we assume the inertial reference frame.

2.1 Stator and Rotor Problems Formulation for Topology Optimization

Usually, the domain of stator and rotor fluidic devices problems may consist of three distinct sub-domains related to: fluid (Ω_f), rotatory solid (Ω_α) and stationary solid (Ω_β). Classical fluid topology optimization literature simulate solid regions as porous material with low permeability (Borrvall and Petersson, 2003). In addition, we also adopt a recently proposed method by Moscatelli *et al.* (2022) that distinguishes each solid domain by adopting two binary design variables (α and β) and modelling their permeability $\kappa(\alpha)$ and $\kappa(\beta)$ separated. Table 1 presents the mapping relating the combination of each discrete value of design variables and each domain. In this work we are only interested on three phases, so we identified the fourth combination as an undesired phase.

Table 1: **Design variables and element phases map.**

α	β	Element phase
1	0	Phase 1 (Rotor)
0	0	Phase 2 (Fluid)
0	1	Phase 3 (Stator)
1	1	Undesired phase

The fluid particle motion is modelled assuming the following conditions: i) constant density ρ and dynamic viscosity μ; and ii) absolute velocity $\mathbf{v}$ and pressure P fields independent of time. The Darcy's law is applied to indicate the regions where the fluid is free or restricted to flow (solid sub-domains). the incompressible rotational Navier-Stokes equations combined with Darcy's term in the inertial reference frame can be written as:

$$\rho\left(\mathbf{v}\cdot\nabla\mathbf{v}\right) = -\nabla P + \mu\nabla^2\mathbf{v} - \kappa(\alpha)(\mathbf{v} - \Omega r) - \kappa(\beta)\mathbf{v}, \tag{1}$$

$$\nabla\cdot\mathbf{v} = 0, \tag{2}$$

where Ω is the rotor speed, r is the radial coordinate, and $\kappa(\alpha)$ and $\kappa(\beta)$ are, respectively, the inverse permeability fields of the porous media for rotor and stator design variables.

In order to aid the derivations on fluid domain, the Darcy material models $\kappa(\alpha)$ and $\kappa(\beta)$ are given by:

$$\kappa(\alpha) = \kappa_{\min} + (\kappa_{\max} - \kappa_{\min})\alpha\frac{1+p}{\alpha+p} \quad \text{and} \quad \kappa(\beta) = \kappa_{\min} + (\kappa_{\max} - \kappa_{\min})\beta\frac{1+p}{\beta+p}, \tag{3}$$

in which $\kappa_{\min}$=0, $\kappa_{\max}$ corresponds to the maximum inverse permeability value ($\kappa_{\max}$=1 kg/m^3.s), and p is the penalty parameter that assumes valor equal to one in binary problems.

3. TOPOLOGY OPTIMIZATION FRAMEWORK

3.1 TOBS-GT for Stator and Rotor Problems

The TOBS-GT method combines seven main features (Picelli *et al.*, 2022): i) decoupled optimization and analysis; ii) binary design variables; iii) smooth contour extraction; iv) geometry trimming; v) sensitivity analysis; vi) numerical filtering; and vii) a branch-and-bound solver. This methodology is implemented via sequential integer linear programming (SILP). In this work we consider stacked up design variables $x = \{\alpha; \beta\}$ and objective function sensitivities $\frac{\partial F}{\partial x} = \{\frac{\partial F}{\partial \alpha}; \frac{\partial F}{\partial \beta}\}$, so the linearized optimization problem to be solved at iteration k may be given by:

$$\begin{aligned} \underset{\Delta \mathbf{x}^k}{\text{Minimize}} \quad & \left.\frac{\partial F(\mathbf{x})}{\partial \mathbf{x}}\right|_{\mathbf{x}^k} \Delta \mathbf{x}^k \\ \text{Subject to} \quad & \text{Minimum Gap Constraint,} \\ & \| \Delta x_j \|_1 \leq \zeta N_d, \quad j \in [1, N_d], \\ & \Delta \alpha_j \in \{S_{\alpha,j}\}, \\ & \Delta \beta_j \in \{S_{\beta,j}\}, \end{aligned} \tag{4}$$

where the linearized objective function $F(\mathbf{x})$ is obtained via the first order Taylor approximation. The flip limits ζ parameter is employed to restrict the maximum flips (changes of discrete values for one state to another, e.g. 0 to 1 and vice versa) as a percentage of total elements in design variables N_d and ensure that the truncation error of the linearization approximation is sufficiently small. Table 2 shows the $S_{\alpha,j}$ and $S_{\beta,j}$ values for updated lower and upper bounds constraints used to identify allowed changes for the steps $\Delta\alpha_j$ and $\Delta\beta_j$.

Table 2: **Bounds constraints for the optimization problem.**

Stacked up design variables			First step		Second step	
α_j	β_j	Element phase	$S_{\alpha,j}$	$S_{\beta,j}$	$S_{\alpha,j}$	$S_{\beta,j}$
1	0	Rotor	{0,0}	{0,0}	{-1,0}	{0,0}
0	1	Stator	{0,0}	{-1,0}	{0,0}	{0,0}
0	0	Fluid	{0,1} or {0,0}	{0,0}	{0,0}	{0,1} or {0,0}

The allowed changes described in Tab. 2 requires the definition of the phases in the boundaries (first elements neighbors of each element). In summary, the allowed changes are separated in two steps regarding which solid domain can be expanded and, consequently, which can be retracted (as can be seen in Fig. 2). We highlighted each element phase with a different color: red (rotor), light blue (fluid) and black (stator). For first step: the rotor elements are maintained in the current state; the fluid elements near the rotor could flip to rotor or be maintained as fluid; and finally, the stator elements can be maintaned as stator or turn to fluid phase. For second step the allowed changes are analogous to the first step, but considering opposite phases expansion and retraction. In addition, the minimum gap constraint restrain that solid elements appear on fluid path if rotor and stator minimum distance is already achieved.

(a) Rotor expansion and stator retraction step

(b) Stator expansion and rotor retraction step

Figure 2: **Two steps optimization to satisfy minimum gap constraint.**

The SILP is solved via a branch-and-bound algorithm implemented in CPLEX optimization library. This method has been used for topology optimization computations for several applications like: 3D microstructural optimization, fluid-structure interaction and thermoelastic problems (Picelli *et al.*, 2020). The SILP solver is used to find the optimal change $\Delta\mathbf{x}$ for the integer design variables $\mathbf{x}$. After each iteration, the design variables are updated as $\mathbf{x}^{k+1} = \mathbf{x}^k + \Delta\mathbf{x}^k$.

3.2 Topology Optimization Problem

In this work we are interested in designing fluid flow paths with maximum energy dissipation, aiming to provide innovative designs to rotating machinery devices. More particularly, the seals are mechanisms projected focusing on leakage reduction. This effect may be achieved by maximizing the absolute energy dissipation composed by viscous and both solids porosity dissipation, given by:

$$F(\mathbf{v}, x) = \int_{\Omega_f} \left(\frac{1}{2}\nu||\nabla\mathbf{v} + \mathbf{v}^T||^2 + \kappa(\alpha)||\mathbf{v} - \Omega r||^2 + \kappa(\beta)||\mathbf{v}||^2 \right) \cdot 2\pi r \, dA. \tag{5}$$

On the proposed approach, both solid regions α and β will be trimmed out of the analysis, so the porosity friction terms will be computed only in the fluid domain.

This optimization problem trivial solution is a closed channel, that is unfeasible as the intention of the device is operating with fluid flowing between the rotor and stator. Therefore, we adopt a minimum gap constraint in order to avoid the closed channel solutions. This constraint is implemented as Moscatelli *et al.* (2022) by defining two neighbourhoods (V_1 and V_R) of each element to control the allowed phases transitions depending of the phases included in each region. Figure 3 illustrates first and R bounds neighbors elements, in which R represents the number of elements imposed as the minimum distance among rotor and stator phases.

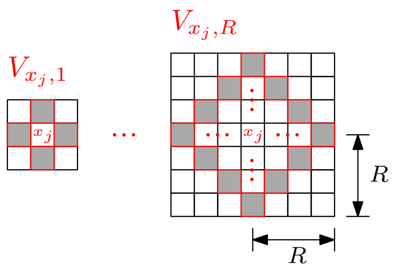

Figure 3: **Neighbours regions used.**

4. Computational Details

In summary, the algorithm of the proposed method is the following:

1. Define the optimization parameters.
2. Create the optimization grid and assign an initial stacked up {0,1} topology.
3. Extract the smooth topology contour and save holes as CAD files.
4. Define the 2D swirl fluid flow problem in CAD and create initial geometry.
5. Trim both rotor and stator solids and fluid holes and create the fluid topology in CAD for Fluid-flow module.
6. Mesh the trimmed geometry according to physics convergence requirements.
7. Solve the governing equations and compute objective function and its both derivatives.
8. Extract (interpolate) each sensitivity field in a grid coincident with the optimization grid.
9. Apply spatial filtering on the sensitivity field considering the optimization grid position.
10. Solve the linearized optimization subproblem with the branch-and-bound algorithm, considering rotor expansion and stator retraction.
11. Update design variables to build a new topology.
12. Repeat steps 3 to 9.
13. Solve the linearized optimization subproblem with the branch-and-bound algorithm, considering stator expansion and rotor retraction.
14. Update design variables to build a new topology and verify the convergence criteria.
15. If converged, stop. If not, iterate from step 3.

In this work, steps from 4 to 8 are carried out in COMSOL Multiphysics, while the others are done in MATLAB using the TOBS implementation available at www.github.com/renatopicelli/tobs. The sensitivity analysis is performed via automatic differentiation. Finally, we leave the software to mesh freely based on physics convergence requirements. We use by default triangular elements for fluid (P2+P1 - quadratic an linear basis for velocity and pressure fields, respectively). However, quadrilateral elements may appear on fluid domain near the fluid walls (boundary layers) in order to provide an accurate approximation of problem geometry.

5. NUMERICAL RESULTS

This section demonstrates the capabilities of the current methodology to maximizing energy dissipation subjected to a minimum gap between the stator and rotor for 2D swirl flows. The fluid is considered to be an oil ($\rho = 835.2$ Kg/m^3 and $\mu = 1.4 \cdot 10^{-2}$ Pa.s) in laminar regime. Convergence is evaluated by the average of the objective function changes over 10 consecutive iterations, with a tolerance $\tau = 0.001$. In this example, we aim to find the optimum fluid flow path between stator and rotor parts of a unit from a labyrinth seal. The fluid enters the channel from the bottom edge with a parabolic profile in tangential direction and semi-parabolic in axial direction, and exits with zero pressure on fluid outlet. The inlet is assigned to the lower port to emphasize that the upward flow (oil leakage) is undesired. The geometric properties and boundary conditions are presented in Fig. 4. The channel units are in mm, and aspect ratio $\delta = 1.6$. Notice that the design domain is selected as the chamber between inlet and outlet, and have the rotor (left edge) and stator (part of bottom and upper edges, and right edge) walls.

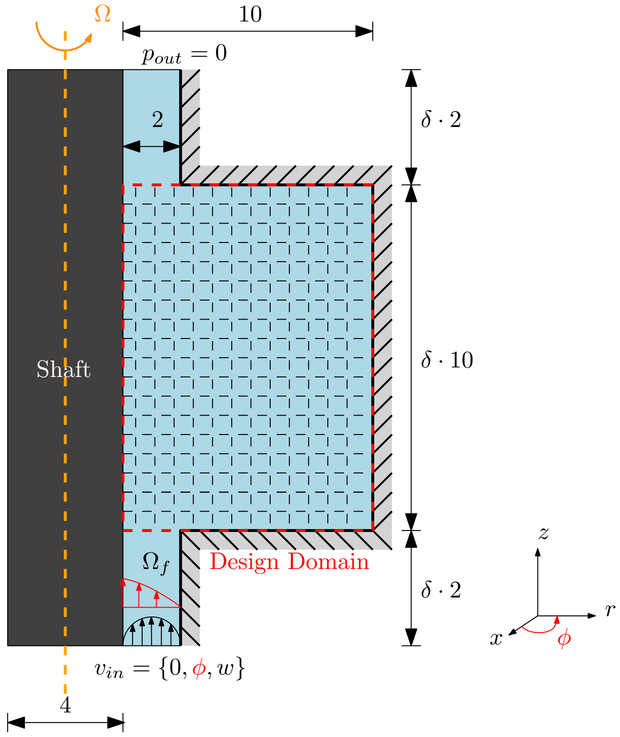

Figure 4: **Laminar seal example with oil.**

We assumed Re=10, $\Omega = \{100, 250, 500\}$ rpm and a 100x160 optimization grid is used for the design domain. In respect to optimization parameters, the flip limit parameter as $\zeta = 0.005$, a filter radius of 5 elements, and a minimum gap of 2 mm (20 elements) were adopted. Figure 5 presents the topologies obtained for several rotational speeds with rotor and stator geometries remarked respectively in red and black colors.

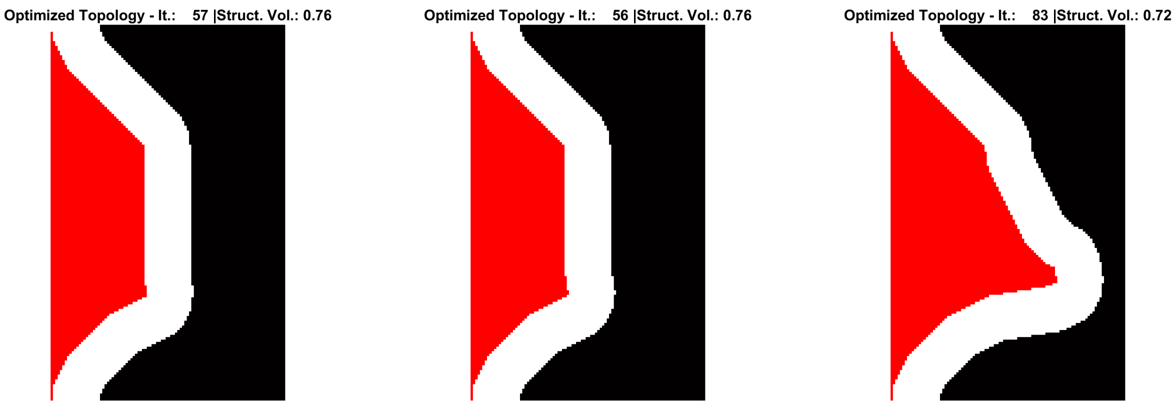

(a) Ω=100 [rpm] (b) Ω=250 [rpm] (c) Ω=500 [rpm]

Figure 5: **Rotations influence in fluid path design on seal for laminar regime.**

Observe in Fig. 5 that the proposed methodology converged for a wide range from lower to higher rotational speeds.

However, as the rotational speed increases, more solid material is redistributed near the inlet of channel forming a sharp tooth on rotor surface. The objective values for the values for the three rotational speeds have been listed in Tab. 3.

Table 3: **Cross-check between objective function and rotational speed for the designs optimized for each velocity.**

Design	Evaluated for		
Optimized for	Ω=100 [rpm]	Ω=250 [rpm]	Ω=500 [rpm]
Ω=100 [rpm]	$1.2511\cdot10^{-4}$ [W]	$2.3371\cdot10^{-4}$ [W]	$6.3371\cdot10^{-4}$ [W]
Ω=250 [rpm]	$1.2552\cdot10^{-4}$ [W]	$2.3498\cdot10^{-4}$ [W]	$6.3290\cdot10^{-4}$ [W]
Ω=500 [rpm]	$1.5267\cdot10^{-4}$ [W]	$3.7634\cdot10^{-4}$ [W]	$1.2213\cdot10^{-3}$ [W]

Notice that the best performance topology is remarked on Tab. 3 for each initial set up for shaft speed. In this particular case, the topology obtained for $\Omega = 500$ rpm was the design with higher energy dissipation among all designs considered. This indicates that for the set ups investigated in laminar regime, the rotor tooth provides a significant dissipation related to its length.

In order to illustrate the final design performance in laminar flow, we focus our discussions considering Re=10 and Ω=500 rpm. Figure 6 presents the: a) velocity magnitude profile [m/s], b) pressure field [Pa] and the convergence history of the energy dissipation. Observe that the geometry solved in FEA is a smoothed version of the jagged geometry of binary design of Fig. 5-c with the solid parts trimmed out of the analysis. The smoothing is carried out by using the Savitzky-Golay filter (Savitzky and Golay, 1964).

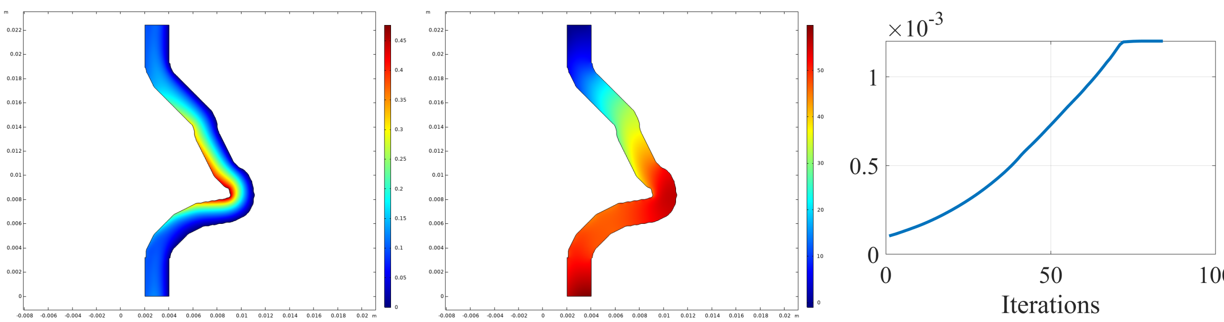

(a) Velocity magnitude (b) Pressure field (c) Convergence curve

Figure 6: **Seal example results for Re=10 and Ω=500 rpm.**

Notice that the maximization of energy dissipation presented a smooth evolution, as can be seen in Fig. 6-c. Also, the velocity magnitude plot presents the highest values in the rotor tooth. This indicates that the tangential speed (ϕ component) dominates the problem when compared to axial (z) and radial (r) velocities. Figure 7 shows the three velocity components of the 2D swirl flow on the final design.

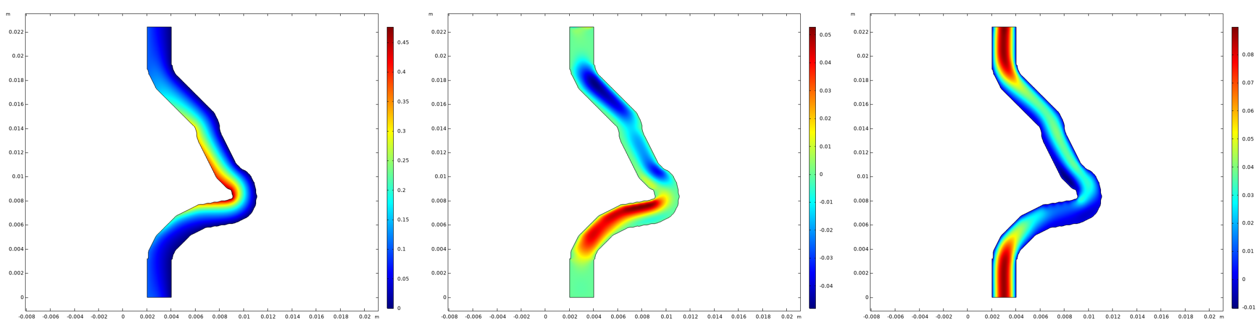

(a) Tangential speed (b) Radial speed (c) Axial speed

Figure 7: **Speed components of 2D swirl flow.**

The sensitivity fields regarding each design variable α and β, and the filtered sensitivities are presented in Fig. 8. Observe that by using this dual design variables formulation, the sensitivities of each solid (rotatory and stationary) can be tracked separately. This is particularly useful to lead with rotor and stator problems, but in theory can be adapted to perform optimization to rotating machinery devices with two distinct rotational speed and no solid at rest.

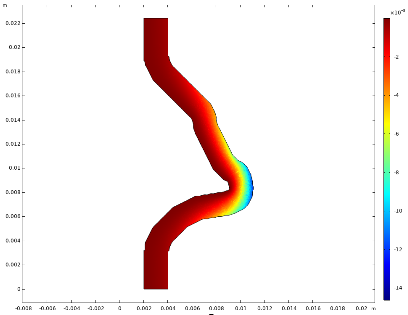

(a) $\dfrac{\partial F}{\partial \alpha}$

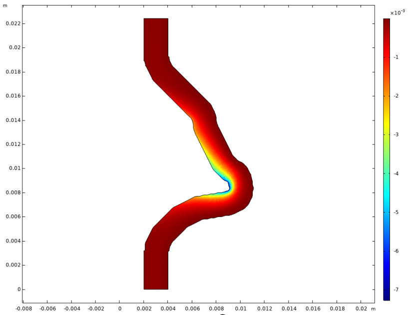

(b) $\dfrac{\partial F}{\partial \beta}$

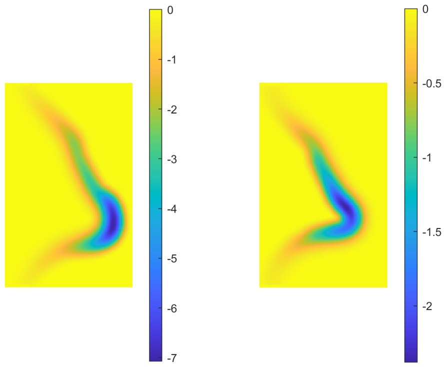

c) Filtered sensitivities

Figure 8: **Sensitivity fields of final seal design.**

Figure 9 shows the velocity profile on a revolved geometry, in order to provide insight of seal device in 3D domain, and the local dissipation in the final fluid path. The local energy dissipation plot reveals that the front of rotor tooth is the main region which contributes to energy dissipation on the optimum topology achieved.

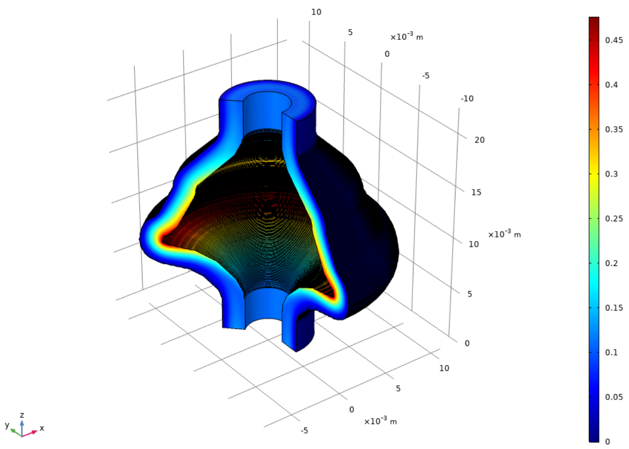

(a) Velocity magnitude in revolved geometry

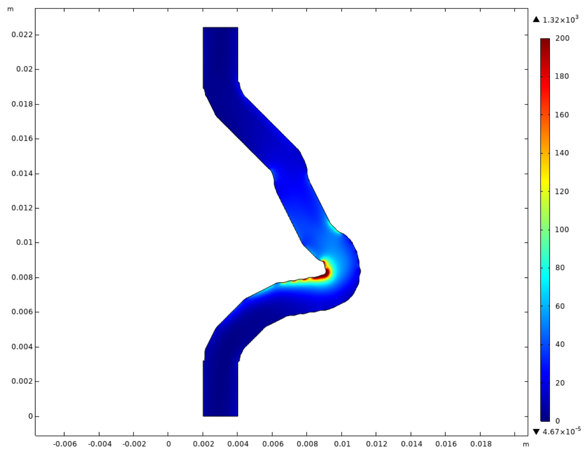

(b) Local energy dissipation

Figure 9: **3D Seal design velocity profile and local energy dissipation field.**

6. CONCLUSION

This paper demonstrated the TOBS-GT implementation applied to the 2D-swirl fluid flow problems considering rotor and stator components via a two design variables approach. We considered laminar flow aiming to maximize energy dissipation subjected to a minimum gap between rotatory and stationary component. It was observed that the rotational speed influences the final design for the fluid path creating a sharp tooth in the rotor while cavities appear on the stator. Numerical results show that the TOBS-GT method has potential to obtain innovative designs of rotating machinery devices considering laminar fluid flow.

7. ACKNOWLEDGMENT

The first author thanks the financial support of FUSP (University of São Paulo Foundation) project number 371065. The second author thanks FAPESP (São Paulo Research Foundation) under grant 2021/02340-0. The fourth author thanks the financial support of CNPq (National Council for Research and Development) under grant 302658/2018-1. The last author would like to thank the support of FAPESP, grants 2018/05797-8 and 2019/01685-3. We gratefully acknowledge support of the RCGI – Research Centre for Greenhouse Gas Innovation, hosted by the University of São Paulo (USP) and sponsored by FAPESP (2014/50279-4 and 2020/15230-5) and Shell Brasil, and the strategic importance of the support given by ANP (Brazil's National Oil, Natural Gas and Biofuels Agency) through the R&D levy regulation.

8. REFERENCES

Borrvall, T. and Petersson, J., 2003. "Topology optimization of fluids in Stokes flow". *International Journal for Numerical Methods In Fluids*, Vol. 41, pp. 77–107.

Fraczek, D. and Wróblewski, W., 2016. "Validation of numerical models for flow simulation in labyrinth seals". *Journal of Physics: Conference series*, Vol. 760, No. KKMP2016, pp. 1–10.

Moscatelli, E., Alonso, D.H., Sá, L.F.N., Picelli, R. and Silva, E.C.N., 2022. "Topology optimisation for rotor-stator fluid flow devices". *Structural and Multidisciplinary Optimization*, Vol. 65: 142.

Picelli, R., Moscatelli, E., Yamabe, P.V.M., Alonso, D.H., Ranjbarzadeh, S., Gioria, R.S. and Silva, J.R.M.E.C.N., 2022. "Topology optimization of turbulent fluid flow via the tobs method and a geometry trimming procedure". *Structural and Multidisciplinary Optimization*, Vol. 65: 34.

Picelli, R., Ranjbarzadeh, S., Sivapuram, R., Gioria, R.S. and Silva, E.C.N., 2020. "Topology optimization of binary structures under design-dependent fluid-structure interaction loads". *Structural and Multidisciplinary Optimization*, Vol. 62, pp. 2101–2116.

Savitzky, A. and Golay, M.J.E., 1964. "Smoothing and differentiation of data by simplified least squares procedures". *Anal Chem*, Vol. 36, pp. 1627–1639.

Sivapuram, R. and Picelli, R., 2018. "Topology optimization of binary structures using integer linear programming". *Finite Elements in Analysis and Design*, Vol. 139, pp. 49–61.

Souza, B., Yamabe, P.V.M., Sá, L.F.N., Ranjbarzadeh, S., Picelli, R. and Silva, E.C.N., 2021. "Topology optimization of fluid flow by using integer linear programming". *Structural and Multidisciplinary Optimization*, Vol. 64, pp. 1221–1240.

9. RESPONSIBILITY NOTICE

The authors are the only responsible for the printed material included in this paper.